Primljen / Received: 18.6.2015.
Ispravljen / Corrected: 17.9.2015.
Prihvaćen / Accepted: 12.10.2015.
Dostupno online / Available online: 10.11.2015.

Analysis of vertical pressure load exerted on horizontal RC plates by wave impact

Authors:

Assist.Prof. Goran Lončar, PhD. CE
University of Zagreb
Faculty of Civil Engineering
Water Research Department
goran.loncar@grad.unizg.hr

Assist.Prof. Dalibor Carević, PhD. CE
University of Zagreb
Faculty of Civil Engineering
Water Research Department
car@grad.hr

Assist.Prof. Damir Bekić, PhD. CE
University of Zagreb
Faculty of Civil Engineering
Water Research Department
damir.bekic@grad.hr

Professional paper

Goran Lončar, Dalibor Carević, Damir Bekić

Analysis of vertical pressure load exerted on horizontal RC plates by wave impact

The analysis of dynamic pressure load exerted on the caisson structure bottom cover plate subjected to wave action is presented and illustrated by the example of Zagreb Pier in the Port of Rijeka. In addition to physical model measurements, empirical models are applied using input data from the linear wave theory and numerical model. The reliability of the applied methodology is assessed through comparison of measured and modelled values. The best correspondence between the measured and modelled results is obtained using the linear wave theory and the Kaplan's (1995) empirical model.

Key words:
wave forces, horizontal plate, physical model, numerical model

Stručni rad

Goran Lončar, Dalibor Carević, Damir Bekić

Analiza vertikalnog tlačnog opterećenja horizontalne armiranobetonske ploče pri udaru valova

U radu se analiziraju tlačna dinamička opterećenja na donju pokrovnu plohu kesonske konstrukcije pri djelovanju valova na primjeru zagrebačke obale u luci Rijeka. Osim mjerenja na fizikalnom modelu, primijenjeni su empirijski obrasci s ulaznim podacima iz linearne teorije valova i iz numeričkog modela. Usporedbom izmjerenih i modeliranih vrijednosti procijenjena je pouzdanost primijenjenih metodologija. Najbolje slaganje modelskih rezultata s izmjerenima postignuto je primjenom linearne valne teorije i empirijskog obrasca prema Kaplanu (1995).

Ključne riječi:
sile valova, horizontalna ploča, fizikalni model, numerički model

Fachbericht

Goran Lončar, Dalibor Carević, Damir Bekić

Analyse vertikaler Drucklasten auf horizontalen Stahlbetonplatten bei Wellenaufprall

In dieser Arbeit werden dynamische Drucklasten auf die untere Deckenfläche von Kesselkonstruktionen unter Welleneinwirkungen am Beispiel der Zagreber Küste des Hafens in Rijeka analysiert. Außer Messungen am physikalischen Model wurden empirische Verfahren mit auf der linearen Wellentheorie und dem numerischen Model beruhenden Eingangsparametern angewandt. Aufgrund einer Gegenüberstellung gemessener und modellierter Werte wird die Zuverlässigkeit der angewandten Methoden beurteilt. Die beste Übereinstimmung der Resultate wurde bei Anwendung der linearen Wellentheorie und des empirischen Verfahrens nach Kaplan (1995) erzielt.

Schlüsselwörter:
Welleneinwirkungen, horizontale Platte, physikalisches Model, numerisches Model

1. Introduction

Wind waves during flow through complex coastal caisson construction types (figure 1) experience significant deformation, primarily through diffraction mechanism around and reflection from piers, as well as viscous displacement and wave break. The effect of changes of wave heights within the construction may result in heaving of the water surface up to the bottom of the cover plate and the appearance of impulsive pressure load. Such pressures act locally, have short duration, and have magnitudes above hydrostatic pressures [1]. Whilst overall stability of the cover construction will not be endangered by this localised activity, it is however important to define the areas on which such an impulsive load appears [2].

Related researches on this topic were initiated as theoretical – mathematical discussions which proved to be relatively accurate in comparison with experimental results obtained from physical two-dimensional models [4]. Vergagen [5] expanded a theoretical-mathematical model by including the influence of air compression. Pioneering research of vertical forces on a flat plate due to monochromatic waves was carried out by El Gharmy [6] on a physical model. Denson and Priest [7] carried out laboratory research of impulsive pressure action on horizontal thin plate with the variation of incidental wave height and of vertical distance between calm sea level and plates. For a similar analysis Broughton and Horn [8] used a physical model made in 1:50 scale, along with variation of plate geometry. Shih and Anastasiou [9] and Toumazis et al. [10] analysed wave-induced pressure loading on horizontal plates by using large scale physical models, and derived basic empirical equations with input parameters in the form of wave height and vertical distance between calm sea level and the plate. A significant contribution to the formation of a theoretical model was made by Kaplan [11]. Isaacson et al. [12] found dimensionless relations between vertical force, wave height, wave period, wave length, water depth, wave steepness and plate geometry. More recently, Tirindelli et al. [13] as well as Cuomo et al. [14] have presented research results from a physical model which aims to define the relationship between quasi-statistic and impulsive pressures on front and central parts of the plate. Laboratory investigations on the appearance of impulsive pressures under plates, with particular focus on compression influence, were carried out in 2009 on a physical model in a scale similar to nature and the research results were published in the work of Martinelli et al. [15]. Araki and Deguchi [16] analysed, on a physical model, the relationship between quasi-statistic and impulsive pressures in conditions of extensive variations of water depth under plates and compared them to the empirical relationship by Cuomo et al. [14]. The results of the above studies served in the adoption of appropriate basic functions within the development of design recommendations [17, 18].

The aim of this paper is to investigate the reliability of the application of various theoretical models for the assessment of impulsive forces from waves on a horizontal plate, by comparing results from physical and numerical models. This study primarily demonstrates the results of laboratory measurements (on a physical model) of impulsive pressure loading on the cover plate caisson construction of a container terminal (figure 1, Zagreb Pier – Port of Rijeka [19]). The designed caisson construction (figure 1) has considerably more complex geometric characteristics and wave field under the cover plates than constructions tested in previously listed references. Therefore the question arises of the reliability of simply applying complex empirical functions for the calculation of vertical loading on the horizontal cover plates. Furthermore, the measured pressures on the physical model represent a reference point, and a comparison to the analytical-empirical model and numerical-empirical model results is used for the reliability assessment of each methodology applied. It should be noted that the primary drawback of physical model results is that they present measurements in only some points. In this way insight into continuous spatial distribution of pressures on the bottom of the cover plate is not gained.

2. Project construction and wind wave features

The desired development of container traffic in the port of Rijeka is to be achieved by the construction of new operating areas. The location of the planned works is Zagreb Pier – Rijeka Harbour (figure 1), in an area 700 m long along the coastline and 180 m wide (perpendicular to the coastline). The designed cover construction will be realised by concrete plates, lying on a series of concrete caissons placed in lines (along the coast) and columns (perpendicular to the coast). Armour layer will be placed between the caisson columns to dissipate wave energy (figure1). A previous study of deep-water wave climate in the area [20] provided basic inputs for the analysis of the action of gravitational sea waves on the construction. Spectral wave parameters for critical incidental wave directions from that previous study (figure 1) were used as boundary conditions in physical and numerical model tests.

3. Physical model

The physical model was constructed from wood in 1:35 scale, according to Froude similarity principles (figure 2). Tests were conducted in a flume with a wave generator which moves a 6m wide plate. The physical model comprises 3 characteristic "longer" constructional sections with 5 rows of caissons as well as 4 "shorter" sections with 2 rows of caissons (figure 2).

In hydraulic modelling practice waves are generated mechanically, where piston type wavegenerator is preferred among other types since orbital wave velocity is simulated more accurately. Wave spectrum generation is based on a technique of superimposing sine waves of different heights and frequencies into the wave spectrum. For the purpose of this

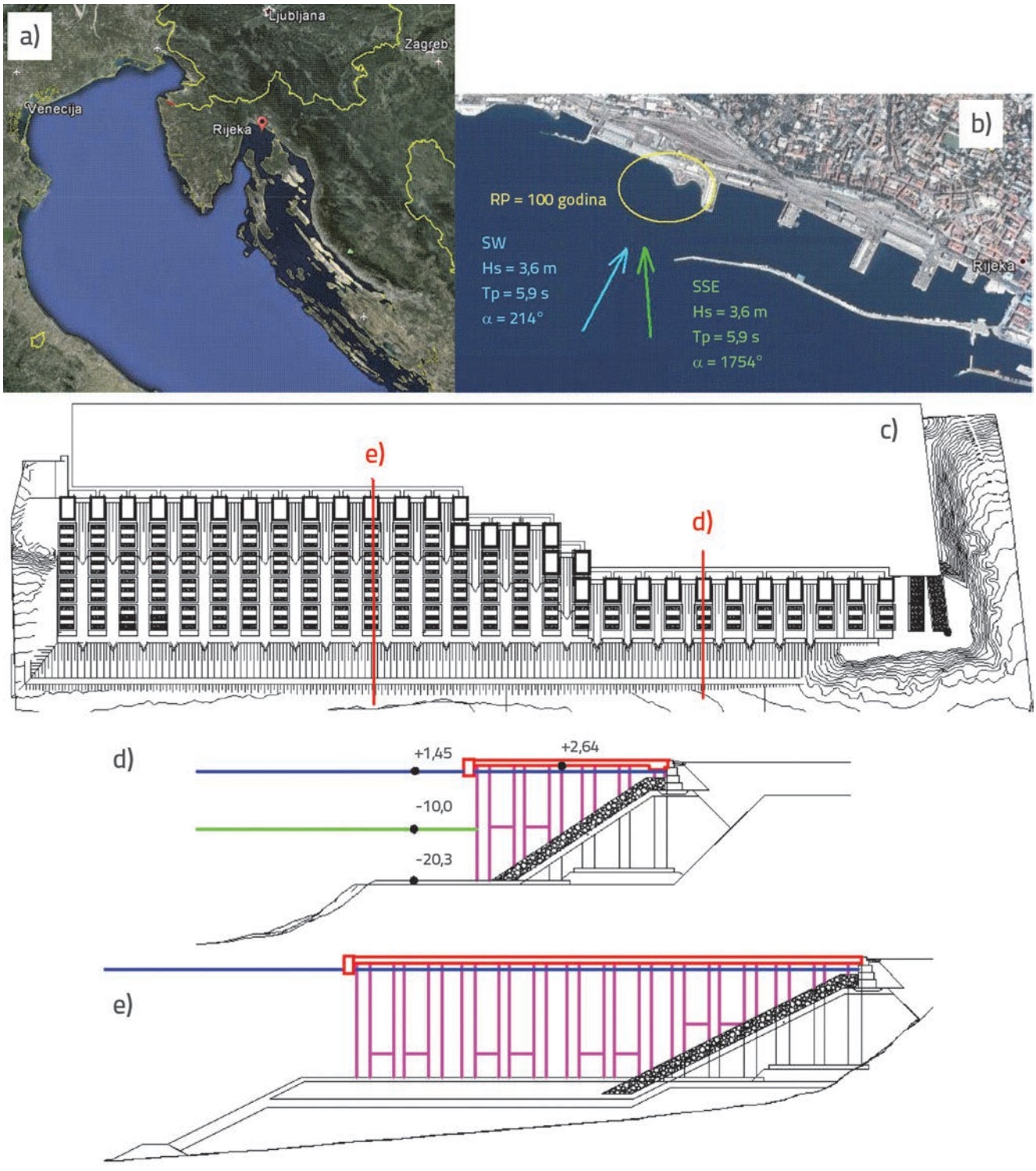

Figure 1. Location of planned works (a,b) with critical directions and appropriate deep-water wave parameters of 100-year return period (b) as well as horizontal (c) and vertical cross-section (d,e) through construction

model scale investigation electro-mechanical piston type wave generator was used. It was capable of generating following types of waves: regular waves (Stokes 1st order, cnoidal and solitary); Irregular waves (Pierson-Moskowitz, Jonswap, ISSC, TMA, Adriatic spectrum) and reproduction of recorded waves. These investigations were conducted using Jonswap wave spectrum (γ = 3.3, σ_1 = 0.07, σ_2 = 0.09). Wave generator consisted of two modules (sections), each having dimensions l x b x h = 3.00 x 2.07

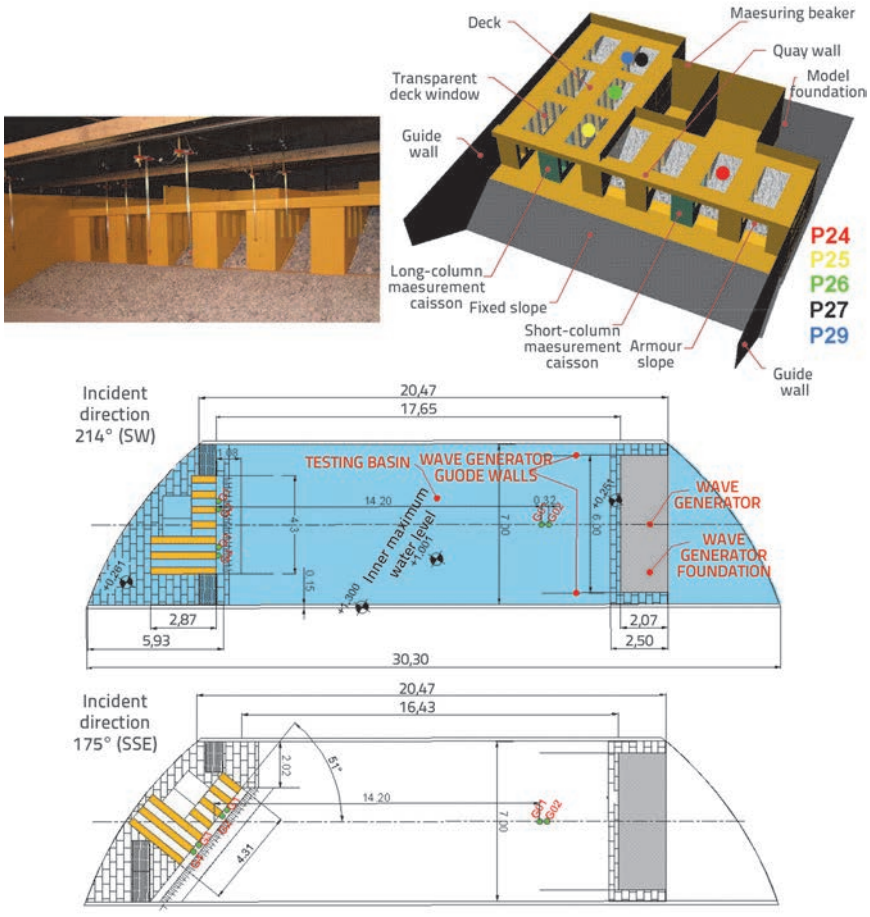

Figure 2. Physical model and spatial positions of measuring equipment

x 0.85 m, ensuring total length of 6 m when placed next to each other. Each module had independent mechanical construction, drive and control unit, and it was operated by computer. Two-dimensional wave field was generated approximately 600 m from the structure in deep water conditions, which was more than recommended minimum 5 - 6 wavelengths for all wavelengths in the spectrum.

Incidental wave spectra were monitored with 2 wave probes G01 and G02 (figure2), measuring the water surface changes at two points: at a distance of 2 characteristic wave lengths from the wave generator panel and at 14 m from the model itself (500 m in prototype scale). Capacitive probes G1 to G4 (figure2) were placed in a line parallel to the outer contours of the construction at a distance of 0.1 m. Probes G2 and G4 were placed in front of the caisson columns, and probes G1 and G3 in front of the entries into the tunnels between the caisson columns. Recorded time series of water surface changes served for the definition of spectral density function by applying the Fourier transformation. Significant wave heights *Hs* were derived from measured energy spectra for each position of measuring probes. The separation of incidental and reflective wave fields was enabled by measurements at probes G01 and G02 by the application of Goda's procedure [21]. The peak wave periods were obtained by spectral analysis. For the data acquisition from capacitive probes a 40 Hz frequency sampling was used. The duration of each test was 10 minutes (1 hour in real time) and that comprised a sufficient number of wave periods (c. 600) for the appropriate modelling of stochastic spectral natural process [27].

Pressure loadings on the bottom of the cover construction were monitored during the conditions of high spring tide (+1.45 m n.m). The positions of 5 Honeywell pressure gauges 26PCBFA6D (P24 to P29) in the physical model are shown in figure 4. The sampling frequency was 1 kHz.

Table 1 shows the reflection coefficients obtained by measurements at probes G1 to G4 for the incidental directions SW and SSE. Figure 3 shows the sequence of measured time series of water surface level at G1 and G3 and the corresponding time series of measured pressures at positions P24 to P27 for the incidental direction SW. Figure 4 gives the same display for the incidental direction SSE. The highest measured pressures at positions P24 to P29 are shown in table 2.

Results in figures 3 and 4 show that the appearance of the highest wave heights in front of the construction correspond with the appearance of the highest pressure under cover plates, which will be used as guidelines in the numerical model implementation and the treatment of results.

Table 1. Reflection coefficients obtained by measurement at probe positions (G1 to G4)

	K_R			
direction	**G1**	**G2**	**G3**	**G4**
SW	0.23	0.30	0.26	0.29
SSE	0.25	0.28	0.26	0.28

Table 2. Highest measured pressures at positions P24 to P29

	P_{MAX} [kPa]			
direction	**P24**	**P25**	**P26**	**P27 / P29**
SW	26.7	22.3	21.6	21.8
SSE	21.7	18.4	21.2	21.4 / 21.8

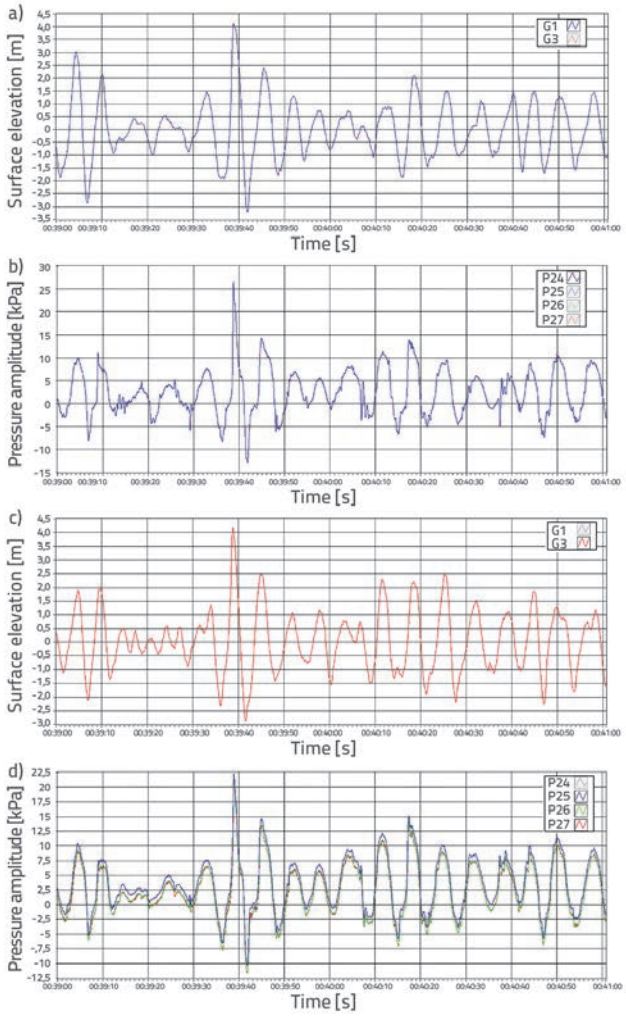

Figure 3. Sequence of measured time series of water surface level (a,c) at measuring probes G1 (a) and G3 (c) and corresponding time series of measured pressures (b,d) at positions P24 (b), P25 to P27 (d) for the incidental direction SW

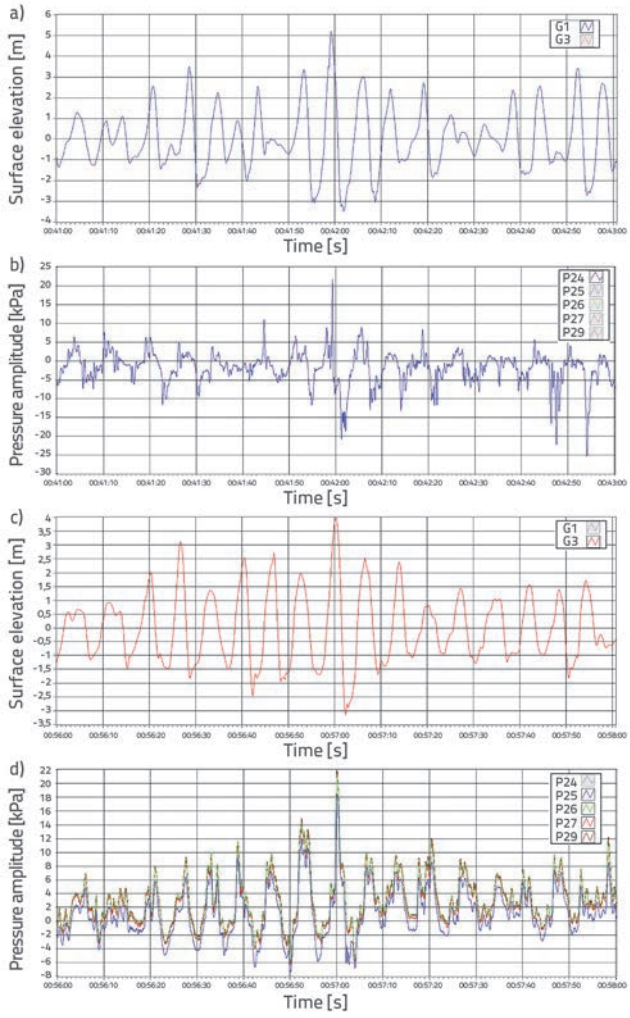

Figure 4. Sequence of measured time series of water surface level (a,c) at measuring probes G1 (a) and G3 (c) and corresponding time series of measured pressures (b,d) at positions P24 (b), P25 to 27 (d) for the incidental direction SSE

4. Empirical models

4.1 Kaplan (1995)

Kaplan [11] focussed his research on finding an empirical model for calculating pressures and forces from wave impact on flat horizontal plates. Total load is expressed by a combination of inertial drag and buoyancy forces. For the definition of vertical component he uses Morison's equation and recognises that the relationship between the vertical distance from water surface to the bottom of the plate and the wave height has a primary role in the strength of impulsive pressures. The proposed empirical term states:

$$p_{kap} = \rho \frac{\pi}{8} \frac{l}{\left[1+(l/b)^2\right]^{-1/2}} \alpha_w + \rho \frac{\pi}{4} c \frac{1+\frac{1}{2}(l/b)^2}{\left[1+(l/b)^2\right]} w + \frac{\rho}{2} C_d w|w| + \rho g a \quad (1)$$

where: ρ is sea density (adopted 1028 kg/m^3), b is width of plate perpendicular to direction of wave propagation (adopted 12.3 m), l is length of plate in direction of wave propagation (adopted 12.3 m), a is thickness of plate (adopted 1.2 m), c is speed of wave propagation, a_w is vertical component of particle acceleration in surface streamline, w is vertical component of particle velocity in surface streamline, C_d is drag coefficient (adopted 2 towards [11]). For the implementation of term (1) it is necessary to determine kinematic parameters c, w and a_w. Their values are calculated with equations (2,3,4), taken from linear wave theory [22]. Thereby, for the wave amplitude the value of $\eta_S = H_S / 2 = 1.8$ m is adopted (half significant wave height of incident spectra of SW and SSE directions), for wave period $T = T_p = 5.9$ s. Vertical components of velocity w and acceleration a_w in terms 3 and 4 are defined for the moment at which the wave profile reaches the plate bottom at +2.64 m, along with the water surface level at +1.45 m (η = 2,64 - 1,45 = 1,19 m).

$$c = gT/2\pi = 9{,}2 \ \text{m/s} \quad (2)$$

$$w = A\omega\frac{\sinh(k(h+z))}{\sin(kh)}\cos(\omega t - kx) = 1{,}44 \ \text{m/s} \quad (3)$$

$$\alpha_w = -A\omega^2\frac{\sin(k(h+z))}{\sin(kh)}\sin(\omega t - kx) = -1{,}34 \ \text{m/s} \quad (4)$$

The designation $k = 2\pi / L$ is a wave number, and $\omega = 2\pi / T$ is wave frequency. By this approach the wave overflow is omitted as well as several components of wave deformations, that appear with the wave arrival at (and in its passage through) caisson constructions (reflection from fender beams and caisson columns, diffraction and reflection inside caisson constructions). By using *c, w* and a_w values from terms (2, 3, 4) into term (1) one obtains the pressure of p_{kap} = 22.1 kPa.

4.2. USACE (2006) and DNV (2010)

In design recommendations and guidelines [17, 18] a simple equation is proposed for the calculation of average pressures p_{dnv} on the plate bottom exposed to wave action:

$$p_{dnv} = C_{dnv}\rho\frac{\omega^2}{2} \quad (5)$$

As in the previous case, the term (5) uses the vertical component of velocity *w* at the moment of wave contact with the plate bottom. For the same condition of water surface level and wave profile as in the previous approach one obtains the value *w* = 1.44 m/s. For the coefficient C_{dnv} the recommended value of 10 is adopted [18].

The practical application of term (5) is immanent in that the obtained p_{dnv} value represents an average pressure on "wetted" plate surfaces. The calculation procedure is described in more detail in the paper [18]. By multiplying the average pressure p_{dnv} and the "wetted" plate area $A_{dnv,}$ the total vertical force on the plate is obtained for the calculation of stability.

Meng [23] proposed the value of the ratio between the average pressures p_{dnv}, relevant for calculation of maximum vertical force on the plate, and the impulsive pressures p_{mng} which appear locally, to be p_{mng} / p_{dnv} = 2. It is important to mention that according to reference [23] the highest pressures appear at the front of the plate. By using values of w = 1.44 m/s, C_{dnv} = 10 and p_{mng}/p_{dnv} = 2 the calculated impulsive pressure is p_{mng} = 21.3 kPa.

4.3. Cuomo (2007)

Cuomo [14] proposes the application of empirical models (6, 7, 8) for the definition of quasi-statistic (6, 7) and impulsive pressures (8) in relation to the incidental significant wave heights H_s and the vertical distances between surface water levels and plate bottom c_r. On the basis of the laboratory research results [14] the two terms proposed were the positions at front-external parts of plates (6) and middle-internal parts of plates (7).

$$p_{cuo-ST} = \rho g H_S\left(2{,}31\left(\frac{\eta_{max} - c_l}{d}\right) + 0{,}05\right) \quad (6)$$

$$p_{cuo-ST} = \rho g H_S\left(0{,}83\left(\frac{\eta_{max} - c_l}{d}\right) + 0{,}13\right) \quad (7)$$

$$p_{cuo} = 2{,}26 p_{cuo-ST} - 0{,}0438 \quad (8)$$

The maximum amplitude of incidental waves is defined by the adopted relationship between maximum and significant wave heights H_{MAX}/H_S = 1.8. For both analysed incidental directions the value of H_S = 3.6 m, and by using the ratio of H_{MAX} / η_{max} = 2 one obtains the value of η_{max} = 3.24 m. The level of the plate bottom is at +2.64 m and the water surface level is at +1.45 m, which gives c_l = 1.19 m. For the water depth *d* the value of *d* = 20 m is adopted. By applying the terms (6,7,8) one obtains the value of impulsive pressures at the front-external part of the plate $p_{cuo(EXT)}$ = 23.1 kPa and the value of $p_{cuo(INT)}$ = 17.3 kPa for the middle-internal part of the plate.

5. Numerical model of wave deformations

The spatial domain of the numerical model was developed to include the extent and disposition of the same caisson construction section as in the flume of the physical model (figure 2 and figure 5). The location of a line of wave spectrum generation in the numerical model is identical to the position of the wave generator in the physical model (in prototype scale) respectively located at an equal distance from the profile of the tested structure. A unidirectional wave spectrum is applied at the line of wave generation in the numerical model, as in the case of the physical model. An equidistant spatial grid was used in the numerical model with the spatial increment $\Delta x = \Delta y$ = 1 m. Hereby a parameterisation-calibration of the numerical model was enabled, with the aim of achieving appropriate levels of reflection, transmission and dissipation. The water depth in the numerical flume is constant (10 m), except at the location of the armour layer where a graded bed of 2V:3H was used as defined in the project documentation. Therefore, the numerical model enables interpretation of wave spectrum for components with length greater than *L* = 20 m (minimum wave period T_{min} = 3.58 s). The adopted hypothesis is that the "lost" part of the wave spectrum with waves of periods less than 3.58 s will not cause significant distortion of wave deformation results in the area of the caisson under the plate. Except for that, the energy of real wave spectrum for the period $T < 3.58$ s is in the model completely shifted to the area of the wave spectrum with $T > 3.58$ s. This implies that the appropriate area below spectrum for periods $T < 3.58$ s is linearly spread on the part of spectrum for periods $T > 3.58$ s. In that way the significant wave height value is preserved despite the reduction of the spectrum.

The developed model is two-dimensional in a horizontal direction and it is not performing direct analysis of the impact

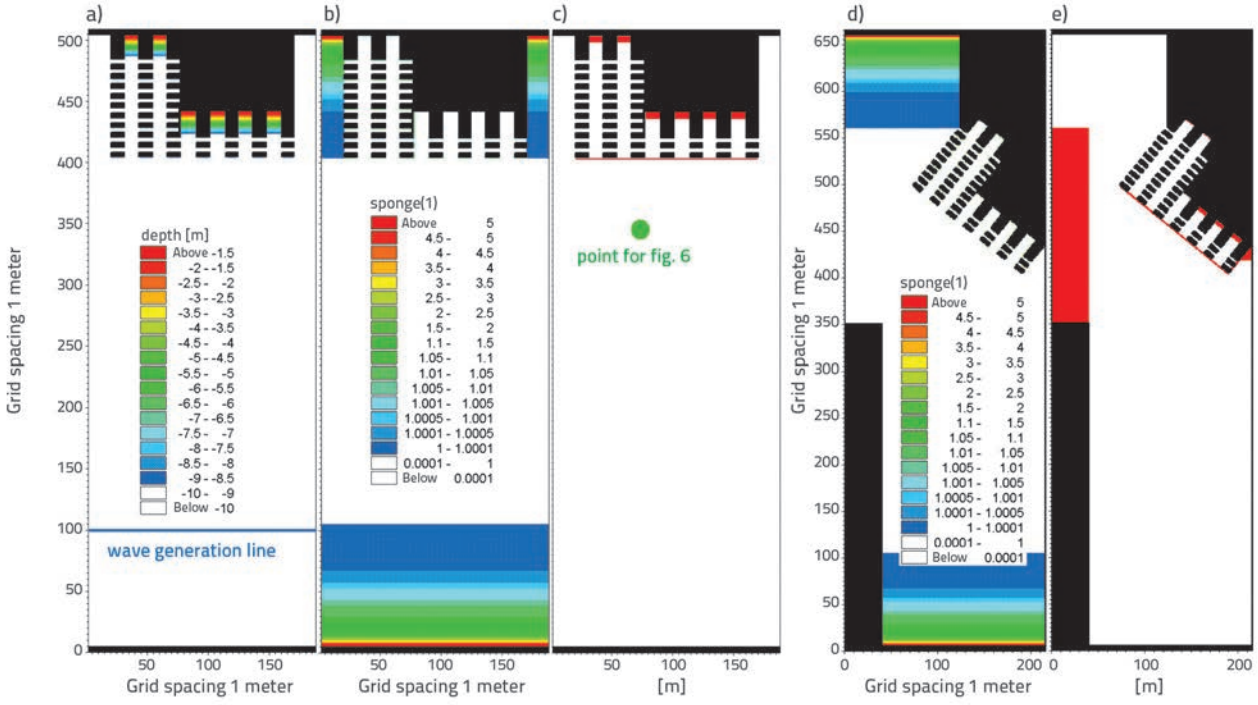

Figure 5. Spatial domain of numerical flume (a), absorptive numerical layers (b,d) and reflexive-transmissive-dissipative numerical layers with appropriate porosity coefficients for SW (c) and SSE (e) incidental wave direction

of cover plates on wave deformations with subsequent distribution of pressures on the cover plate bottom. Thus, the horizontal RC cover plate is not defined as a boundary condition. The numerical simulation provided unsteady and complex 2D field of sea level changes in the zone of the caisson (under the plate). The vertical component of velocity w and acceleration a_w for the wave particle profile at the moment of reaching the level of +2.64 m (the bottom of the cover plate) are calculated from that 2D field and by using an external numerical routine. The corresponding impulsive pressures are obtained by the application of empirical models presented in the preceding chapter. Beside the positions of the pressure gauges P24 to P29, additional positions were monitored at which the sea level periodically reaches the level of +2.64 m. In this manner it is possible to more rationally estimate overall cover plates on which impulsive loading acts as well as optimal sizing of constructions. The intention in the numerical modelling is to ensure appropriate similarity to the reflection and dissipation characteristics of the caisson structure. These characteristics were obtained by measurements on the physical model. The desired level of the reflection and/or dissipation of wave energy in the spatial domain of the numerical model was accomplished by using the sponge layers and the porosity layers with calibrated numerical coefficients (figure 5). Absorbent layers disable the wave reflection from wall boundaries of the numerical model which are not present in reality, and disable the wave energy spreading outside the area of primary interest. The principle variables which are varied in the model parameterisation are the porosity coefficient, coefficients of laminar and turbulence resistance as well as the size of the solid particle of porous composites.

During the passage over caisson construction, the incident wave energy is partially reflected from the wall and fender beams, partially transmitted under the fender beam in the caisson zone and also partially lost in the process of overflow. A loss of incidental wave energy during overflow is estimated by the coefficient of transmission due to overflow [24]. By such an approach, the calculated coefficient of transmission due to overflow is $K_{TP} = 0.18$. The coefficient of transmission under the fender beam (in the caisson zone) is estimated with the value $K_{TP} = 0.8$ [25]. If a conservative form of the relationship between incidental, reflective and transmitted energy is adopted, then the following term is valid for coefficients $K_T^2+K_{TP}^2+K_R^2 = 1$. Such an approach also defines the reflection coefficient of $K_R = 0.2$ for the part of the construction in front of the spaces in between the caisson columns (for example for the position of measuring probe G3). Given that the analysed complex structure also has dissipative characteristics, a slightly reduced value of $K_R = 0.15$ is applied in the numerical model. On the other hand, the enhanced reflection appears in front of the caisson columns (position of measuring probe G4) and in the numerical simulation the value of $K_R = 0.45$ was used. The average reflection coefficient value of $K_R = 0.3$ was used in the numerical model for the entire area in front of the fender beams. Similar values were also obtained in the physical model tests (average value $K_R = 0.27$, (see table 1).

The investigation of the wave field and wave deformation dynamics was conducted in the numerical model Mike 21/BW (www.dhigroup.com). The numerical model Mike 21/BW is based

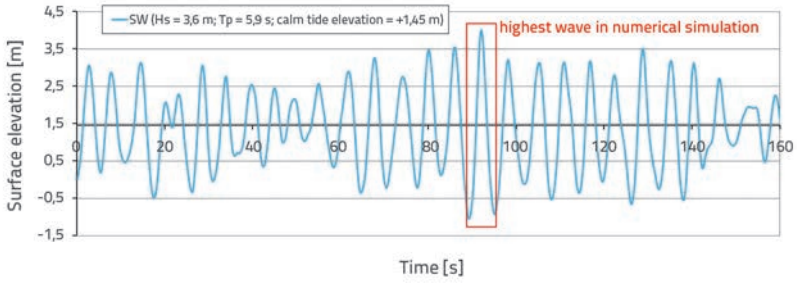

Figure 6. Sequence of sea level at a point in front of the caisson construction (JONSWAP spectrum; γ = 3.3; HS-PP5 = 3.6 m; TP = 5.9 s)

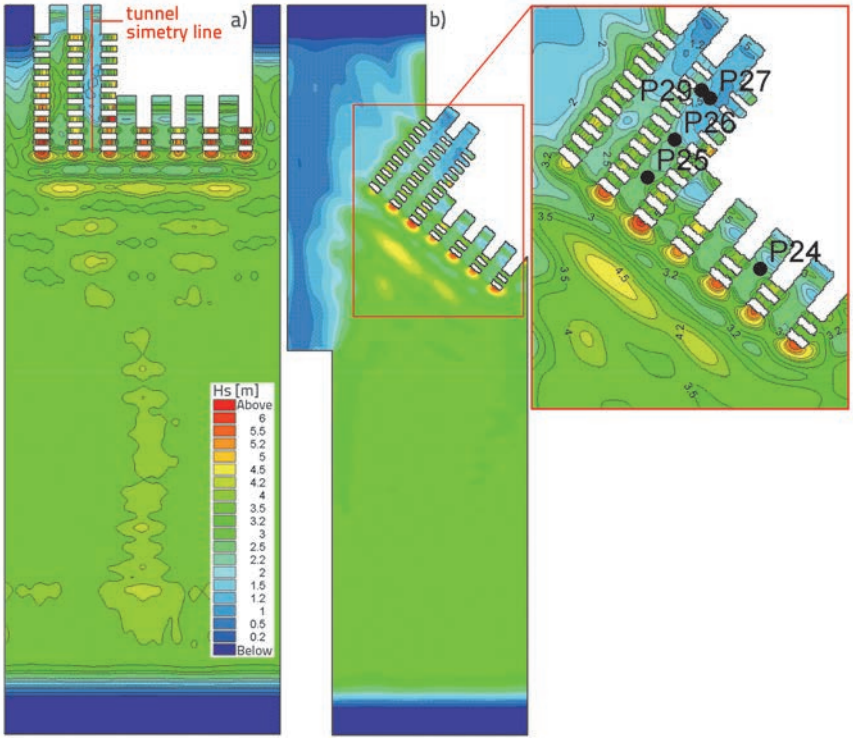

Figure 7. Fields of significant wave height for SW (a) and SSE (b) incidental direction waves

Table 3. Calculated values of the vertical component of velocity *w* and acceleration a_w for particle of wave profile at the moment of reaching the cover plate bottom (level +2.64 m), at positions P24 to P29

w [m/s]				
direction	P24	P25	P26	P27 / P29
SW	1,76	1,53	0,4	1,08/2,04
SSE	1,44	1,72	1,93	0,5/1,01
a_w [m/s^2]				
smjer	P24	P25	P26	P27 / P29
SW	-0,034	-0,032	-0,031	-0,024/-0,031
SSE	-0,024	-0,032	-0,029	-0,03/-0,036

on the resolving of the time domain in Bousinesq's equations. These equations contain members that comprise the influence of frequency dispersion and non-linearity. The effect of frequency dispersion and the effect of vertical acceleration on pressure distribution are also included in momentum equations. The equations are resolved by using flux-formulations (velocity x water depth) with improved linear dispersion characteristics [26]. The implicit solution of differential equations is used in the numerical model. This numerical model includes all combinations of relevant impacts on wave deformation such as refraction, diffraction, bottom friction, partial reflection and transmission, non-linear interaction between two or more waves and frequency spread, as well as non-linear phenomena such as the formation of higher and lower harmonics. A reference [26] gives a detailed overview of the numerical formulations of the numerical model Mike 21/BW.

As the physical model results show that the largest wave from the wave series produces the greatest impulsive load, attention in numerical modelling was directed towards the propagation of the highest wave through the caisson construction. Figure 6 shows a time sequence of sea levels at one point in front of the construction (see figure 5) for incidental direction SW (JONSWAP spectrum; γ = 3.3; H_s = 3.6 m; T_p = 5.9 s). The resulting fields of significant wave height H_s for incidental waves SW and SSE are shown in figure 7.

The speed of wave propagation *c* in the caisson construction zone is calculated by the tracking of wave ridges along the centre line of the tunnel between the adjacent lines of caisson columns (see figure 7). The average propagation speed was *c* = 6.3 m/s. Figure 8 shows the profile of wave propagation in the centre line of the tunnel with 1 second shift.

Table 3 gives the calculated values of the vertical components of velocity *w* and acceleration a_w for the particle of wave profile at the moment of reaching the bottom of the cover plate (level +2.64 m), at the position of the pressure gauges P24

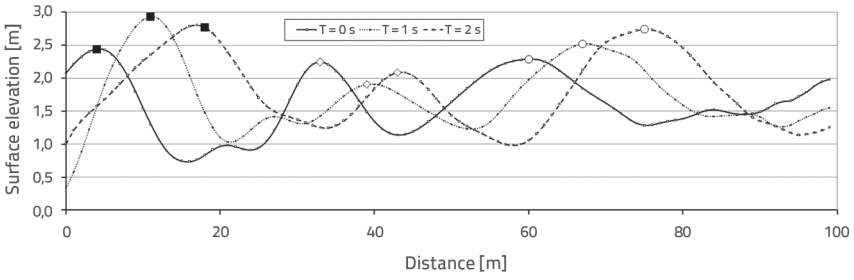

Figure 8. Wave propagation profile in centre line of tunnel with 1 second shift

to P29. Figure 9 shows the corresponding values of impulsive pressures according to the empirical terms from chapter 4, and by applying values of *c*, *w* and a_w from the numerical model. It should be noted that the presented pressure values are for the highest wave from the total 30-minute simulation period.

Figure 10 presents positions at which sea level simultaneously reaches a level of +2.64 m (bottom of plate). This enables assessment of the total impulsive load on the overall cover plate. Figure 11 shows a time series of the total surface area with impulsive pressure action during the passage of the highest wave from the simulated period.

If it is assumed that the measured pressures on the physical model are the most reliable, the reliability of applied approaches can be assessed by statistical parameters of the average error

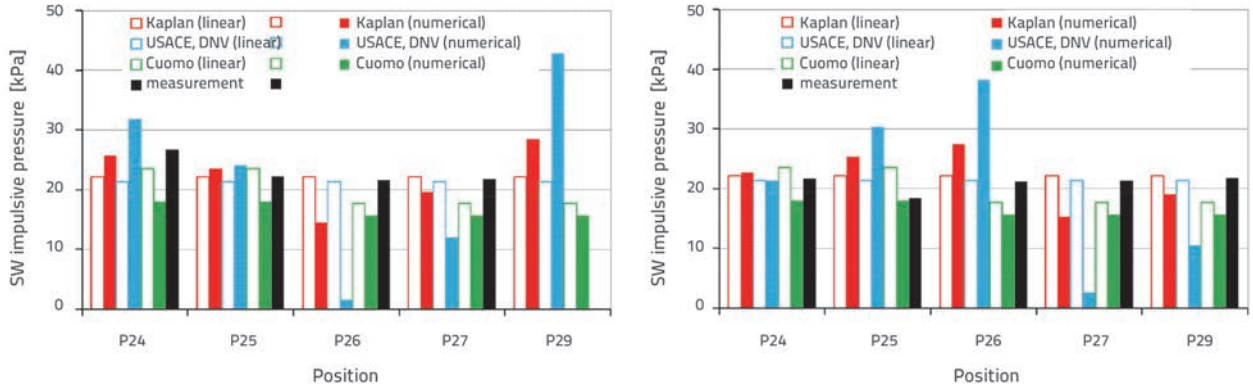

Figure 9. Maximal impulsive pressures measured at pressure gauges P24 to P29 as well as calculated pressures by empirical terms from chapter 4, along with the application of values *c*, *w* and a_w from linear wave theory (chapter 4) and the results of numerical simulation (this chapter)

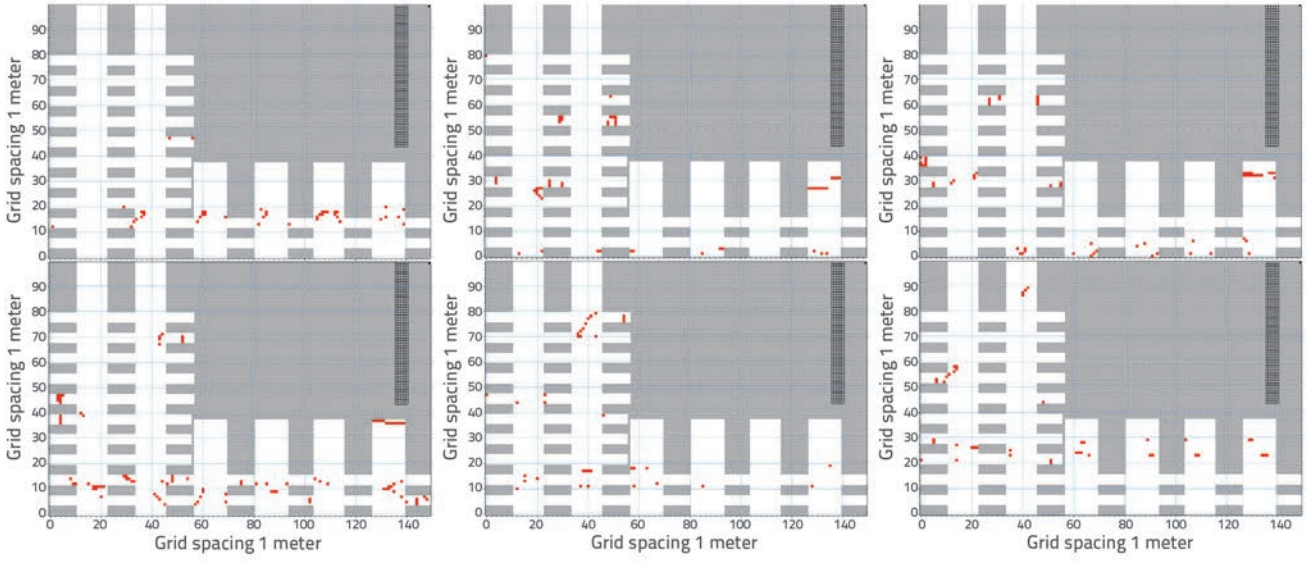

Figure 10. Positions (red marks) on which sea level simultaneously reaches a level +2.64 m (bottom of plate) during the passage of the highest wave from the simulated period (SW incidental direction)

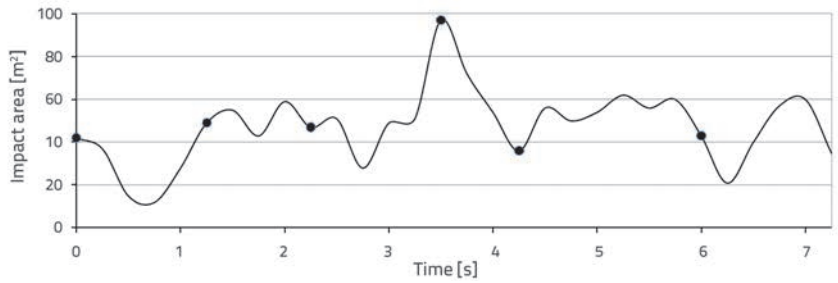

Figure 11. Time series of total surface area with impulsive pressure action during the passage of the highest wave from the simulated period (SW incidental direction). At marked points the layouts in figure 10 are given.

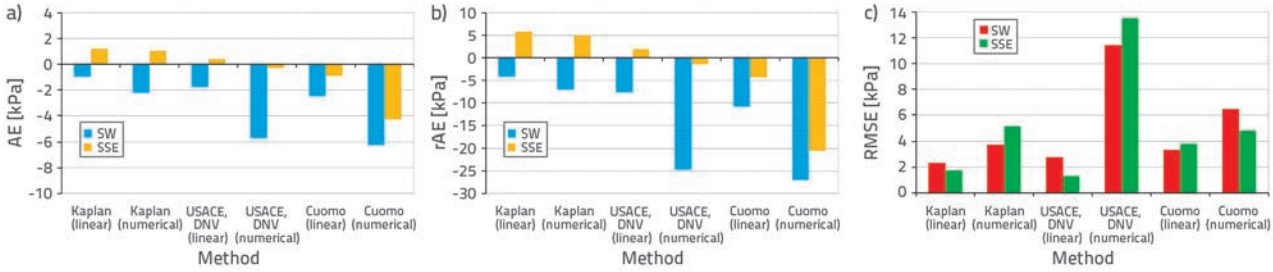

Figure 12. Average error *AE* (a), relative average error *rAE* (b) and root mean square error *RMSE* (c) for variable of impulsive pressure by applied approaches

AE, the relative average error *rAE* and the root mean square error *RMSE* for variable of impulsive pressure (figure 12).

6. Conclusions

The impulsive pressures on surface plates of caisson constructions were analysed under the action of wind waves. The reference values of the impulsive pressures on the bottom of plates were obtained by measurements on the physical model at several positions and for the two relevant wave incidental directions (SW and SSE). The measured values were compared to the calculated values from empirical models. Whereas the applied empirical models assume that the kinematic parameters of wave profile are known, they are initially calculated by using linear wave theory and by using the numerical model results of wave deformations.

A comparison of the modelled and measured results shows the following:

- the application of linear theory for the calculation of kinematic parameters of wave profile allows finding only one value of impulsive pressure, without distinguishing its spatial distribution under surface plates;
- the impulsive pressures appear only locally, and according to the model results less than 1 % of total surface area was simultaneously exposed to the impulsive pressure load;
- the pressures obtained by Kaplan (1995) and DNV (2010) empirical models, and with the application of linear wave theory, have the smallest difference to the measured values;
- the pressures obtained by empirical models with the application of linear wave theory give low average error (*AE*) and low root mean square error (*RMSE*) when compared to the results obtained by empirical models with the application of the numerical model results;
- the average errors (*AE*) are less for the SSE incidental wave direction than for the SW direction;
- for the SW incidental wave direction the average errors (*AE*) are negative for all applied methods. Given this, the calculated values are not on the side of safety. Positive *AE* values were obtained by using the Kaplan (1995) model and for the SSE incidental wave direction;
- the smallest difference between calculated and measured values of impulsive pressures was obtained by using linear wave theory and the Kaplan (1995) empirical model, with the relative average error of *rAE* = 5 %.

It can be concluded that the application of linear wave theory and the Kaplan (1995) empirical term give acceptable engineering assessment of the impulsive pressures on cover plates due to wave action.

REFERENCES

[1] Lai, C.P., Lee, J.J.: Finite Amplitude Wave Uplift on Platforms or Docks, *Journal of Waterways, Ports, Coastal & Ocean Engineering*, ASCE, 115 (1989) 1, pp. 19-39, http://dx.doi.org/10.1061/(ASCE)0733-950X(1989)115:1(1)

[2] Bhat, S.S.: *Wave slaming on the horizontal plate*, A thesisi in parial fulfillment oft he requirements for the degree of master of applied science, The University of British Columbia, 1994.

[3] Wagner, H.: *Landing of Seaplanes*, National Advisory Committee for Aeronautics, Technical Note No. 622., 1932.

[4] Chuang, S.L.: Experiments on slamming of wedge-shaped bodies with variable dead rise angle, *J. Ship Research*, 11(1967) 4, pp. 190-198.

[5] Verhagen, J.H.G. (1967): The impact of flat plate on a water surface, *J. Ship Research*, 11(1967) 4, pp. 211-223.

[6] El Gharmy, O.A.: *Wave force on a dock*, Report no. HEL-9-1, Inst. Of Engg. Research, Hydraulic Engg. Lab., University of California, Berkley, California. 1963.

[7] Denson, K.H., Priest, M.S.: Wave pressure on the underside of a horizontal platform, *Proc. Offshore Technology Conference*, Houston, USA, pp. 555-570, 1971., http://dx.doi.org/10.4043/1385-MS

[8] Broughton, P., Horn, E.: Ekofish Platform 2/4C: Re-analysis Due to Subsidence, *Proc. Inst. Civ. Engrs.*,82 (1987), pp. 949-979, http://dx.doi.org/10.1680/iicep.1987.488

[9] Shih, R.W.K., Anastasiou, K.: A Laboratory Study of the Wave-induced Vertical Loading on Platform Decks, *Proc. ICE, Water Maritime and Energy*, 96 (1992) 1, pp. 19-33, http://dx.doi.org/10.1680/iwtme.1992.18495

[10] Toumazis, A.D., Shih, W.K. & Anastasiou, K.: Wave Impact Loading on Horizontal and Vertical Plates, *Proc. IAHR 89 Conf.*, Ottawa, Canada, pp. 209-216, 1989.

[11] Kaplan, P., Murray J.J., Yu W.C.: Theoretical Analysis of Wave Impact Forces on Platform Deck Structures, *Volume 1-A Offshore Technology, OMAE - Offshore Mechanics and Arctic Engineering Conference*, Copenhagen, pp. 189-198, 1995.

[12] Isaacson, M., Allyn, N., Ackerman, C.: Design wave loads for a Jetty at Plymouth, Montserrat, *International Symposium: Waves-physical and numerical modelling*, University of British Columbia, Vancouver, Canada, pp. 1153-1162, 1994.

[13] Tirindelli, M., Cuomo, G., Allsop, N.W.H., Lamberti, A.: Wave-in-Deck Forces on Jetties and Related Structures, *Proceedings of The Thirteenth International Offshore and Polar Engineering Conference*, Honolulu, USA, pp. 562-569, 2003.

[14] Cuomo, G., Tirindelli, M., Allsop, N.W.H.: Wave-in-deck loads on exposed jetties, *Coastal Engineering*, 54 (2007) 9, pp. 657-679.

[15] Martinelli, L., Lamberti, A., Gaeta, M., Tirindelli, M., Alderson, J., Schimmels, S.: Wave loads on exposed jetties: description of large scale experiments and preliminary results, Coastal Engineering Proceedings, 1(32), structures.18 (2011), doi:http://dx.doi.org/10.9753/icce.v32.structures.18

[16] Araki, S., Deguchi, I.: Prediction of wave force acting on horizontal plate above still water level, *Proceedings of 33rd Conference on Coastal Engineering*, Santander, Spain, pp. 1-12, 2012.

[17] USACE: *Coastal Engineering Manual _ Part 6, Chapter 5, Fundamentals of Design*. 2006.

[18] Det Norske Veritas: *Recommended Practice - Environmental Conditions and Environmental Loads*, DNV-RP-C205, 2010.

[19] Brodarski institute: *Zagreb Container Terminal Pier Structure - Hydraulic investigations on physical model and numerical analysis of the wave field in front of the structure - Final report*, Technical report no. 6359-H, Zagreb, 2013.

[20] Hydroexpert: *Wind and wave climate for the Port of Rijeka – Zagreb Pier*, Technical report, Zagreb, 2013.

[21] Goda, Y., Suzuki, Y.: Estimation of incident and reflected waves in random wave experiments, *Proceedings of 15th International Conference on Coastal Engineering*, Hawaii, pp. 828-845, 1976.

[22] Mei C.C.: *The applied dynamics of ocean surface waves*, Advanced series on ocean engineering, Worl scientific Ed., New Jersey, 1989.

[23] Meng, Y., Chen, G., & Yan, S.: Wave interaction with deck of jetty on a slope Coastal Engineering Proceedings, 1(32), posters.21 (2011), doi:http://dx.doi.org/10.9753/icce.v32.posters.21

[24] Goda, Y.: *Random Seas and Design of Maritime Structures*, Advanced series on ocean engineering, Worl Scientific Ed., New Jersey, 2000.

[25] Wiegel, R.L.: Transmission of waves Past a Rigid Vertical Thin Barrier, *J. of the Waterways and Harbors Division*, ASCE, (1960) 6, pp. 1-12.

[26] Madsen, P.A., Murray, R., Sorensen, O.R.: A new form the Boussinesq equations with improved linear dispersion characteristics, *Coastal Engineering*, (1991) 15, pp. 371-388, http://dx.doi.org/10.1016/0378-3839(91)90017-B

[27] Journée, J.M.J., Massie, W.W., Offshore Hydromechanics, First edition. Delft University of Technology, (2001), pp. 5-43 (http://www.shipmotions.nl).